CORTEX 49 (2013) 200–210

Available online at www.sciencedirect.com

SciVerse ScienceDirect

Journal homepage: www.elsevier.com/locate/cortex

Research report

Hemispheric asymmetries of cortical volume in the human brain☆

Elkhonon Goldberg[a,*], Donovan Roediger[a], N. Erkut Kucukboyaci[a,b], Chad Carlson[a], Orrin Devinsky[a], Ruben Kuzniecky[a], Eric Halgren[b] and Thomas Thesen[a]

[a] New York University School of Medicine, New York, NY, USA
[b] Multimodal Imaging Laboratory, University of California, San Diego, CA, USA

ARTICLE INFO

Article history:
Received 19 June 2011
Reviewed 2 September 2011
Revised 27 September 2011
Accepted 28 October 2011
Action editor Alan Beaton
Published online 19 November 2011

Keywords:
MRI morphometry
Cortical asymmetry
Hemispheric specialization
Prefrontal cortex
Parietal cortex

ABSTRACT

Hemispheric asymmetry represents a cardinal feature of cerebral organization, but the nature of structural and functional differences between the hemispheres is far from fully understood. Using Magnetic Resonance Imaging morphometry, we identified several volumetric differences between the two hemispheres of the human brain. Heteromodal inferoparietal and lateral prefrontal cortices are more extensive in the right than left hemisphere, as is visual cortex. Heteromodal mesial and orbital prefrontal and cingulate cortices are more extensive in the left than right hemisphere, as are somatosensory, parts of motor, and auditory cortices. Thus, heteromodal association cortices are more extensively represented on the lateral aspect of the right than in the left hemisphere, and modality-specific cortices are more extensively represented on the lateral aspect of the left than in the right hemisphere. On the mesial aspect heteromodal association cortices are more extensively represented in the left than right hemisphere.

1. Introduction

Hemispheric specialization is among the central features of functional cortical organization in humans. Recognition of the functional differences between the hemispheres often triggers interest in their morphological differences and vice versa.

Indeed, gross morphological differences between the hemispheres are particularly interesting if they can be related to functional differences. The degree to which such relationships can be drawn remains uncertain, since the relationship between brain biology and function may be expressed on many levels other than that of gross morphology (cytoarchitectonic, biochemical, etc.). Thus any attempt to infer regional brain function from regional brain morphology, however tempting, requires great caution and any assertion of a "bigger is better" structure–function relationship must be tempered by this caveat. Such concerns notwithstanding, evidence is growing that a reasonably direct "bigger is better" relationship often does exist between functional proficiency and gross morphometric cortical characteristics of the underlying

☆ Authors' Note: The study was approved by the Institutional Review Board of New York University. Written informed consent was obtained from all participants involved in the study. We thank Dmitri Bougakov, Barry Cohen, Michal Harciarek, Dolores Malaspina, Ralph Nixon, and Kenneth Podell for their comments.

* *Corresponding author*. NYU School of Medicine, 145 East 32nd Street, 5th Floor, New York, NY 10016, USA.
E-mail addresses: elkhonon.goldberg@nyumc.org, egneurocog@aol.com (E. Goldberg).

0010-9452/$ – see front matter © 2011 Elsevier Ltd. All rights reserved.
doi:10.1016/j.cortex.2011.11.002

substrate, such as regional volume or surface area size (Blackmon et al., 2010; Draganski et al., 2004; Fleming et al., 2010; Maguire et al., 2000; Schneider et al., 2002).

Early efforts to identify morphological hemispheric asymmetries were to a large degree motivated by the desire to identify the biological bases of the asymmetric cortical language representation. A number of morphological asymmetries have been described, notably involving *planum temporale* and *pars opercularis*, and their relationship to left hemispheric dominance for language asserted, but some of the particularly influential findings were reported several decades ago using what methodologies were available then (Geschwind and Levitsky, 1968; Galaburda et al., 1978; LeMay and Culebras, 1972). Subsequent research confirmed these structural asymmetries (Foundas et al., 1994, 1995; Anderson et al., 1999; Watkins et al., 2001) but demonstrated that the relationship between structural asymmetries in the *planum temporale* and language lateralization is not nearly as strong or as direct as asserted earlier, and the very existence of such a relationship has been scrutinized (Beaton, 1997). Other structural asymmetries have also been described and subsequently confirmed, notably "Yakovlevian torque" (Yakovlev, 1972; Yakovlev and Rakic, 1966; Watkins et al., 2001; Narr et al., 2007) characterized by the right frontal and left occipital protrusions, whose possible relationship to any functional asymmetries remains unclear. Regional hemispheric asymmetries both in cortical thickness (Luders et al., 2006) and volume (Good et al., 2001), both in gray and white matter (Penhune et al., 1996; Takao et al., 2011) have been reported.

Any morphometric comparison of the two hemispheres may be complicated by individual variability, which is particularly pronounced in certain structures, e.g., anterior cingulate and paracingulate cortex (Fornito et al., 2004; Huster et al., 2007). Furthermore, there is a growing appreciation of sex-linked differences in regional brain morphology (Witelson, 1989; Habib et al., 1991; Crespo-Facorro et al., 2001), including hemispheric asymmetries (Luders et al., 2009; Raz et al., 2004), as well as age-related hemispheric differences (Raz et al., 2004; Shaw et al., 2009).

Our understanding of the functional differences between the two hemispheres has also been refined beyond the classic distinction between verbal and visuo-spatial asymmetries. Additional functional differences have been described, notably those linking the right hemisphere to cognitive novelty and exploratory behavior and the left hemisphere to cognitive familiarity and routinization. Since this functional asymmetry was first proposed (Goldberg and Costa, 1981; Goldberg et al., 1994a), it has found support with various neuroimaging techniques, including PET (Gold et al., 1996; Shadmehr and Holcomb, 1997), fMRI (Henson et al., 2000), and high-frequency EEG (Kamiya et al., 2002). It has been argued that the "novelty-routinization" functional hemispheric asymmetry is fundamental and irreducible to the more commonly invoked language-visuospatial asymmetry, since it is present in a wide range of mammalian species (Vallortigara, 2000; Vallortigara and Rogers, 2005; Vallortigara et al., 1999).

To account for these functional differences, it has been proposed that systematic differences between the two hemispheres exist in relative cortical space allocation to heteromodal association cortices versus modality-specific cortices (Goldberg and Costa, 1981). If this were to be the case, the functional implications of such cortical space allocation differences could be intriguing and would merit further examination. However, this assertion was based on old findings and was limited to cortical convexity; therefore its validity must be re-examined with up-to-date methods which would target both lateral and mesial aspects of the hemispheres. Here, we report hemispheric differences in regional human brain volume across multiple cortical regions, both lateral and mesial, using the more recently developed FreeSurfer Magnetic Resonance Imaging (MRI) processing methodology (Fischl and Dale, 2000; Fischl et al., 2004). The particular focus of this paper is to ascertain any systematic differences in cortical space allocation to heteromodal versus modality-specific cortices in the two hemispheres.

2. Methods

2.1. Participants

Structural MRI data from adults ($N = 39$) aged 19–40 ($M_{age} = 27.75$, standard deviation – $SD_{age} = 6.12$; 19 females and 20 males) were analyzed. Participants were all right-handed as determined by the Edinburgh Handedness Inventory (Oldfield, 1971) with scores ranging from 40 to 100. They were all free of neurological, psychiatric, or neurodevelopmental disorders based on screening interviews. They were recruited as part of a community-based normative reference sample at NYU Comprehensive Epilepsy Center.

2.2. Imaging data acquisition

Two T1-weighted volumes ($TE = 3.25$ msec, $TR = 2530$ msec, $TI = 1.100$ msec, flip angle = 7°, field of view (FOV) = 256 mm, voxel size = $1 \times 1 \times 1.33$ mm) were obtained for each participant on a 3T Siemens Allegra scanner, acquisition parameters optimized for increased gray/white matter contrast, rigid body co-registered, and common space-reoriented. Images were automatically corrected for spatial distortion, registered, averaged to improve signal-to-noise ratio, and processed with the FreeSurfer (4.0.2) software (http://surfer.nmr.mgh.harvard.edu). Each T1-weighted image took 8:07 min.

2.3. Imaging data processing

Averaged volumetric MRI images were used to model each subject's cortical surface with an automated procedure involving white-matter segmentation, gray/white matter boundary tessellation, inflation of folded surface tessellation, and automatic topological defect correction (Dale et al., 1999; Fischl et al., 2001).

Automated analysis was performed on a 156 node computing cluster and took approximately 32 h per scan. Each analysis was then manually inspected which took, depending on segmentation quality, 20–40 min. Measures of cortical thickness were obtained by constructing estimates of the gray/white matter boundary by classifying all white matter voxels in the MRI volume. The white matter surface was submillimeter accuracy-refined in delineating the gray/white matter

junction. Estimates of cortical thickness were made by measuring (1) the shortest distance from each point on the white matter surface to the pial surface, and (2) the shortest distance from each point on the pial surface to the white matter surface. Cortical thickness at each vertex was computed as the average of the two values. The accuracy of automatic parcellation methods is often undermined by individual variability. For this and other reasons, manual quality inspection was performed on all reconstructions and required manual intervention in 5% of scans. All of these cases were reinspected and all yielded good segmentation results. Maps were smoothed with a Gaussian kernel (10 mm FWHM) across the surface. Cortical surfaces from different individuals were morphed to a common reference brain by aligning sulcal–gyral patterns while minimizing shear and metric distortions (Fischl et al., 1999). Automatic parcellation of the cortical surface was performed with sulco-gyral neuroanatomic labels derived by probabilistic information. Past research has validated these automatic labels against anatomical manual labels and 85% of the surface was found to be concordant (Destrieux et al., 2009, 2010). Parcel regions of interest (ROI) designation as "gyrus" or "sulcus" was based on the values of local mean curvature and average convexity, obtained from the reconstructed cortical surfaces output from FreeSurfer, relative to a given threshold; vertices with values below the threshold were considered sulcal, and vertices with values equal to or above this threshold were considered gyral. A total of 75 ROI were identified in each hemisphere. In each ROI, cortical thickness estimates were averaged across all vertices. Regional volumes were calculated as the product of surface area and average cortical thickness.

For the whole-sample analysis, a laterality index (LI) – as defined by Nagata et al. (2001) – was used to control for sex-linked variability in global brain volume. Regional LI values were calculated for each subject using the following equation:

$$\mathrm{LI} = \frac{\mathrm{Left} - \mathrm{Right}}{\mathrm{Left} + \mathrm{Right}} \times 100$$

This index spans from −100 to 100 with positive values indicating leftward asymmetry, negative values indicating rightward asymmetry, and zero indicating perfect symmetry. For each ROI, a two-tailed single-sample *t*-test was used to compare the distribution of LI values against zero. To maintain an experiment-wise error rate of .05, Bonferroni correction ($\alpha = .00067$) was employed to address the problem of multiple comparisons, where the number of comparisons was 75. In separate analyses by sex, paired-sample *t*-tests were used to compare left and right regional volumes among each pair of contralateral ROIs. An identical Bonferroni correction method was utilized for these pairwise tests. Areas were considered asymmetric if the statistical significance criterion ($\alpha = .00067$) was reached. Reported visualizations map statistical results on the 3D whole brain volume (with the parcel boundaries between the structures exhibiting the same direction of laterality removed for visual clarity).

3. Results

Since we were interested in the relationship between functionally distinctive cortical regions, the analysis has been conducted in terms of ROIs volumes, each derived from cortical thickness measures and surface area parcellation boundaries. We found multiple regional hemispheric asymmetries which are summarized in Fig. 1 and Table 1. In order to highlight the most robust and best articulated patterns of asymmetries, the results and discussion below detail only those asymmetries which remained significant at $p < .05$ level after a rigorous Bonferroni correction for multiple comparisons was applied ($\alpha = .00067$). This correction, which lowers Type I errors at the expense of Type II errors, highlighted the most prominent asymmetries. These are summarized in Fig. 2 and described below. Here we present the result of regional cortical volume comparisons. We found that regional cortical surface comparisons were generally consistent with the volume comparisons Thickness comparisons yielded few significant asymmetries when rigorous statistical criteria were used.

3.1. *Whole-sample asymmetries (males and females combined)*

Fig. 1A shows uncorrected *p* values, while Fig. 2A shows post-Bonferroni significant asymmetries for the whole sample. The superior frontal gyrus, superior frontal sulcus, frontomarginal sulcus, suborbital sulcus, gyrus rectus, postcentral gyrus, postcentral sulcus, cingulate gyrus, paracentral gyrus, subcentral gyrus, transverse temporal gyri, superior temporal gyrus (lateral aspect), planum temporale, superior parietal gyrus, anterior occipital sulcus, ascending ramus of the lateral fissure, and circular insular sulcus (superior and inferior aspects) were larger in the left than right (L > R) hemisphere across the whole sample (all *p* values < .00067). Conversely, the inferior parietal gyrus, superior occipital gyrus, lingual gyrus, calcarine sulcus, lateral fissure (posterior segment), collateral transverse sulcus, middle frontal sulcus, subparietal sulcus, anterior subcentral sulcus, superior temporal sulcus, cingulate sulcus, the lateral aspect of orbital gyri, pericallosal sulcus, and Jensen sulcus were larger in the right than left (R > L) hemispheres (all *p* values < .00067). This is summarized in Fig. 2A, where regions larger in the right hemisphere are depicted in yellow and regions larger in the left hemisphere are depicted in blue.

3.2. *Analyses of sex-linked differences*

When grouped by sex, leftward asymmetries (L > R) of the anterior occipital sulcus and lateral aspect of superior temporal gyrus were significant in females (both *p* values < .00067) but not males ($p > .05$ and $p < .005$, respectively) while the cingulate gyrus, planum temporale, and superior frontal sulcus were significantly larger on the left in males (all *p* values < .00067) but not females ($p < .05$, $p < .005$, and $p < .005$, respectively). Conversely, rightward asymmetry (R > L) of the lingual gyrus occurred in females ($p < .00067$) but not males ($p < .005$) and the subparietal sulcus was significantly larger in the right hemisphere in males ($p < .00067$) but not females ($p < .005$). Notably, the superior temporal and Jensen sulci and the lateral aspect of orbital gyri both failed to reach significance in either sex alone despite displaying significant rightward asymmetry in the

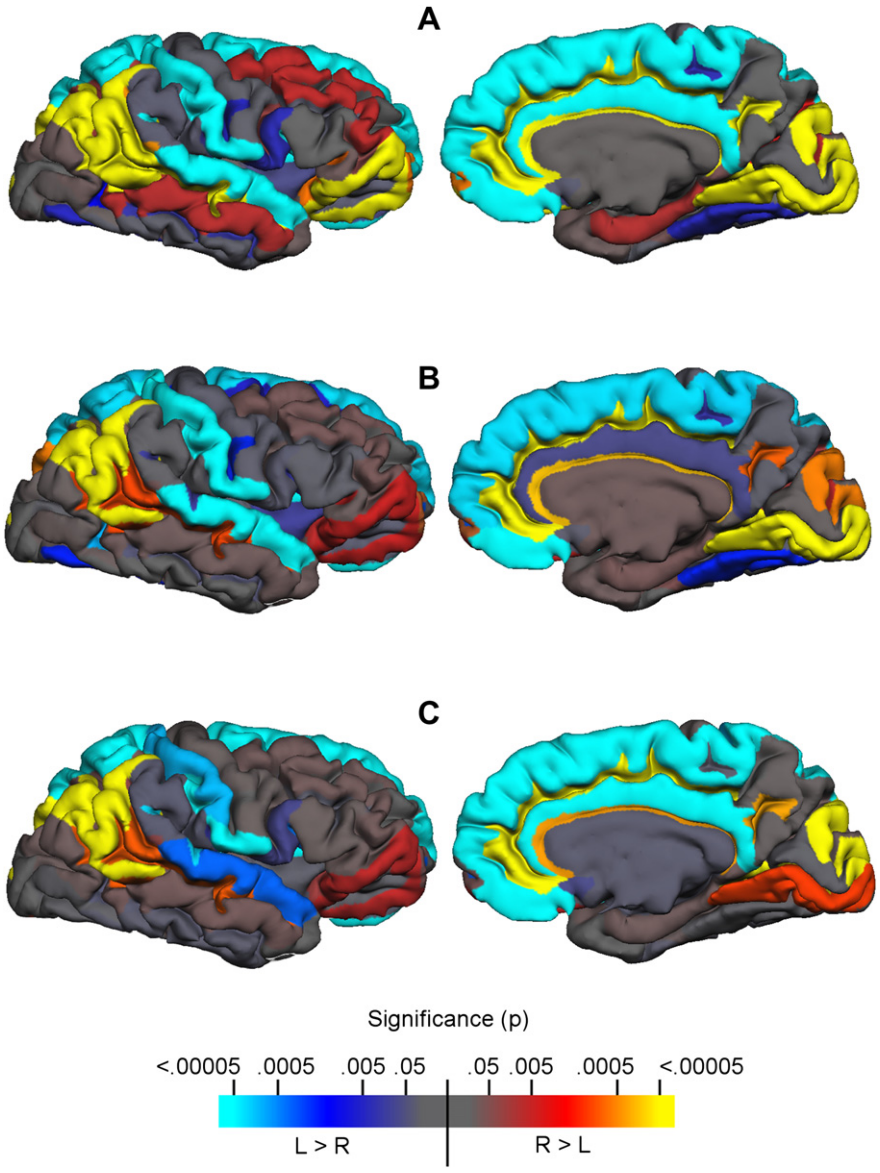

Fig. 1 – Regional cortical volume asymmetries in the two hemispheres uncorrected for multiple comparisons. Direction of differences and uncorrected significance levels are coded according to the color bar below: (A) whole-sample, (B) females only, (C) males only.

whole-sample analysis. No parcels revealed significant laterality in opposing directions across sexes.

Sex-specific results are detailed in Table 2. Fig. 1B and C shows uncorrected *p* values for females and males, respectively, while Fig. 2B and C shows post-Bonferroni significant asymmetries for each sex. Although Figs. 1 and 2 appear to suggest sex differences, an ANOVA failed to reveal significant interactions between sex and laterality in any ROI.

4. Discussion

In this study we intentionally adopted a conservative significance criterion for data analysis, in order to identify a relatively small number of the most robust hemispheric differences while possibly overlooking less robust differences. As a result, several distinct asymmetry patterns emerged, which are discussed below.

4.1. *Heteromodal association cortical asymmetries*

We found differences in the hemispheric representation of heteromodal association cortices. Heteromodal inferoparietal and ventrolateral prefrontal cortices are more extensive in the right than left hemisphere. By contrast, mesial and orbital prefrontal and cingulate cortices are more extensive in the left than right hemisphere. These asymmetries closely parallel the findings by Luders et al. (2006) pertaining to cortical thickness.

Thus it appears that heteromodal association regions found on the lateral (convexital) aspect of the hemisphere, are more extensive in the right than in the left hemisphere, as predicted earlier (Goldberg and Costa, 1981). This is true both for the

Table 1 – Regional volumetric comparisons and LIs [(L − R)/(L + R) × 100] for males and females combined. For each ROI, the means and SDs of right and left hemisphere cortical volume (mm^3) measurements, as well as the means and SDs of LIs, are listed.

ROI	Mean (SD)			Sig.
	Left (mm^3)	Right (mm^3)	LI	
Anterior occipital sulcus	1097.4 (274.3)	895.8 (298.2)	11.07 (17.52)	<.05[a]
Calcarine sulcus	3381.8 (649.1)	3903.7 (709.3)	−7.21 (5.62)	<.05[a]
Central insular sulcus	289.1 (81)	258.5 (72.9)	5.73 (20.7)	n.s.
Central sulcus	3609.6 (492)	3488.8 (633)	1.96 (5.57)	n.s.
Cingulate and intracingulate sulci	6797.9 (956.1)	9525.1 (1372.4)	−16.63 (6.06)	<.05[a]
Cingulate gyrus	4740.8 (968.5)	3979.2 (710.1)	8.44 (11.18)	<.05[a]
Cingulate sulcus (marginalis part)	1332.1 (259.9)	1312.5 (309.3)	1.11 (11.42)	n.s.
Circular sulcus of insula (anterior)	935.5 (153.3)	1050.3 (266.4)	−5.06 (8.77)	n.s.
Circular sulcus of insula (inferior)	2299.2 (332.3)	1908.4 (270.8)	9.22 (5.87)	<.05[a]
Circular sulcus of insula (superior)	2778 (367.8)	2199.3 (324.6)	11.68 (5.8)	<.05[a]
Collateral transverse sulcus (anterior)	1523.3 (388.8)	1673.2 (473.8)	−4.47 (15.35)	n.s.
Collateral transverse sulcus (posterior)	492.8 (155.3)	762.6 (212.9)	−21.3 (16.74)	<.05[a]
Cuneus	3407.2 (547.6)	3399.4 (654.4)	.31 (7.98)	n.s.
Frontomarginal gyrus	1032.2 (290.9)	1196.8 (314.9)	−7.71 (13.01)	n.s.
Frontomarginal sulcus	1006.4 (252.7)	764.5 (190.2)	13.19 (14.95)	<.05[a]
Gyrus rectus	2154.4 (361.5)	1669 (302.1)	12.67 (8.52)	<.05[a]
H-shaped orbital sulcus	2502 (395.1)	2428.2 (401)	1.55 (8.04)	n.s.
Inferior frontal gyrus (opercular part)	3400.2 (653.1)	3150.7 (503)	3.59 (8.45)	n.s.
Inferior frontal gyrus (orbital part)	871 (241.7)	935.2 (233.6)	−4.26 (16.47)	n.s.
Inferior frontal gyrus (triangular part)	2698.4 (453)	2704.8 (546.5)	.18 (9.12)	n.s.
Inferior frontal sulcus	3101.6 (748.6)	2968.4 (479.9)	1.63 (9.78)	n.s.
Inferior occipital gyrus and sulcus	2797 (717.6)	2832.9 (628.7)	−1.05 (12.42)	n.s.
Inferior parietal gyrus (angular part)	5535.6 (868.2)	6946.9 (1132.1)	−11.69 (7.6)	<.05[a]
Inferior parietal gyrus (supramarginal part)	6671.4 (1173.9)	6465.7 (1011.6)	1.39 (6.57)	n.s.
Inferior temporal gyrus	6362.9 (1149.1)	6227 (1315)	.89 (8.09)	n.s.
Inferior temporal sulcus	1972.1 (487.2)	1793.4 (444.1)	4.63 (12.13)	n.s.
Insular gyrus (long)	870.4 (248.7)	874.4 (172.8)	−.84 (9.26)	n.s.
Insular gyrus (short)	1852.7 (326.6)	1776.1 (355.4)	2.38 (7.17)	n.s.
Intraparietal and transverse parietal sulci	3815.8 (522.2)	4022 (579.3)	−2.58 (7.02)	n.s.
Isthmus	351.4 (101.7)	375.3 (100.4)	−3.64 (12.05)	n.s.
Lateral fissure (horizontal ramus)	499 (141.6)	578.6 (124.1)	−7.81 (13.96)	n.s.
Lateral fissure (posterior)	1638 (271.5)	1968.1 (250.6)	−9.34 (7.33)	<.05[a]
Lateral fissure (vertical ramus)	598.4 (166.7)	435.1 (139.5)	15.52 (21.28)	<.05[a]
Lateral occipito-temporal gyrus (fusiform)	4522.4 (751)	4192.5 (804.7)	3.92 (8.47)	n.s.
Lateral orbital gyrus	6260.5 (998.2)	6802.1 (1197.1)	−4.07 (5.4)	<.05[a]
Lateral orbital sulcus	628.8 (200.3)	727.4 (299.4)	−6.1 (17.97)	n.s.
Lingual gyrus	5609.9 (930.2)	6546.4 (960.8)	−7.78 (7.11)	<.05[a]
Medial occipito-temporal and lingual sulci	3187.2 (574.5)	3187.3 (654.1)	.11 (7.95)	n.s.
Medial occipito-temporal gyrus (parahippocampal part)	4242.8 (565.7)	4494.5 (554.2)	−2.91 (7.24)	n.s.
Medial orbital sulcus	913 (149.8)	858.3 (173.4)	3.34 (10.05)	n.s.
Medial wall	5543.4 (1079.9)	5513.1 (733.2)	−2.1 (5.7)	n.s.
Middle frontal gyrus	9632.4 (1944.6)	10211.8 (1836.7)	−3.1 (7.08)	n.s.
Middle occipital gyrus	4411.2 (579.7)	4563 (739.8)	−1.49 (7.36)	n.s.
Middle occipital sulcus and sulcus lunatus	1550 (420.7)	1589 .4 (534.9)	−.32 (17.4)	n.s.
Middle temporal gyrus	8128.8 (1368.6)	8497.4 (1359.7)	−2.29 (5.48)	n.s.
Occipito-temporal sulcus (lateral)	1328.6 (331.5)	1413.6 (338.3)	−3.3 (11.28)	n.s.
Paracentral gyrus	2554.8 (414.5)	2101 (337.4)	9.77 (8.13)	<.05[a]
Paracentral sulcus	318.5 (94.2)	275.2 (84.8)	7.52 (18.39)	n.s.
Parieto-occipital sulcus	2643.4 (541)	2828.1 (496.8)	−3.62 (7.44)	n.s.
Pericallosal sulcus	1303.4 (211.3)	1592.1 (275.5)	−9.88 (9.03)	<.05[a]
Planum polare	1873.4 (387.7)	1950.1 (400.5)	−2.05 (9.81)	n.s.
Planum temporale	2293.3 (493.4)	1887.6 (361.7)	9.35 (11.89)	<.05[a]
Postcentral gyrus	4201.2 (677)	3556.1 (710.2)	8.57 (6.99)	<.05[a]
Postcentral sulcus	3794.8 (648.6)	3006.9 (759.1)	12.13 (8.64)	<.05[a]
Precentral gyrus	6246.9 (825.9)	6211.5 (959.3)	.41 (5.48)	n.s.
Precentral sulcus (inferior part)	2475.8 (571.5)	2615.8 (317)	−3.49 (9.88)	n.s.
Precentral sulcus (superior part)	1933.5 (467.3)	2062.4 (398.2)	−3.58 (11.84)	n.s.
Precuneus gyrus	5724.6 (800.4)	5285.8 (857.5)	−.05 (5.38)	n.s.
Subcallosal gyrus	315.6 (144.3)	256.6 (81.8)	7.29 (30.36)	n.s.

Table 1 – (*continued*)

ROI	Mean (SD)			Sig.
	Left (mm^3)	Right (mm^3)	LI	
Subcentral gyrus	2573.9 (395)	1986.4 (386.4)	13.06 (9.43)	<.05[a]
Subcentral sulcus (anterior)	163.3 (83.8)	287.9 (109.5)	−27.61 (29.22)	<.05[a]
Subcentral sulcus (posterior)	499.5 (148.3)	440 (123.2)	5.92 (16.33)	n.s.
Suborbital sulcus	1007.7 (249.5)	617.1 (185.8)	24.38 (13.13)	<.05[a]
Subparietal sulcus	1694.1 (342.2)	2081.9 (484.4)	−9.78 (10.09)	<.05[a]
Sulcus intermedius primus (Jensen)	546.2 (254)	704.3 (275.5)	−13.65 (22.15)	<.05[a]
Superior frontal gyrus	20151 (2783.3)	18661.6 (2336)	3.75 (2.92)	<.05[a]
Superior frontal sulcus	4794.6 (972.9)	4085.2 (909.9)	7.99 (8.3)	<.05[a]
Superior occipital gyrus	2455.3 (452)	3098.4 (612.4)	−11.34 (8.25)	<.05[a]
Superior occipital sulcus and sulcus transversalis	1649.7 (327.5)	1815.1 (327.8)	−4.82 (10.95)	n.s.
Superior parietal gyrus	5735 (977.9)	4746.1 (718.8)	9.25 (6.23)	<.05[a]
Superior temporal gyrus (lateral aspect)	5907.4 (842.2)	5138.2 (788.9)	7.01 (6.41)	<.05[a]
Superior temporal sulcus	8790.3 (1275.9)	9666.6 (1151.9)	−4.89 (5.61)	<.05[a]
Temporal pole	5607.1 (836.1)	5968.2 (678.1)	−1.07 (6.29)	n.s.
Transverse temporal gyrus and intermediate sulcus	1087.6 (206.2)	840.1 (184.9)	12.94 (9.61)	<.05[a]
Transverse temporal sulcus	531.3 (137.2)	456.7 (100.8)	7.16 (13.78)	n.s.

a After Bonferroni correction for multiple comparisons.

inferoparietal and for parts of the lateral prefrontal regions. By contrast, heteromodal association cortices found on the mesial and orbital aspects of the hemisphere are more extensive in the left than in the right hemisphere. This is true for the mesial prefrontal regions, as well as for the cingulate cortex. The dual dissociation in the volumetric asymmetries of lateral versus mesial heteromodal association cortices is not commonly mentioned in the literature on hemispheric differences, but it

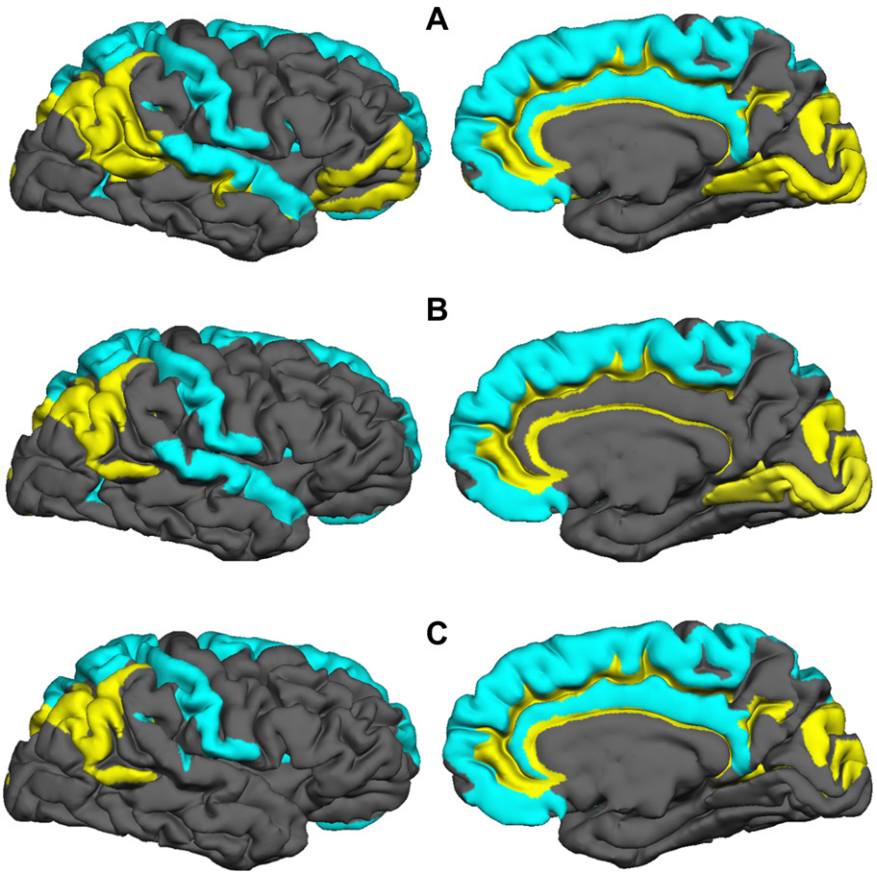

Fig. 2 – Regional cortical volume asymmetries in the two hemispheres corrected for multiple comparisons. Regions significantly larger after the correction ($p < .05$) in the left hemisphere are in blue; regions significantly larger in the right hemisphere are in yellow: (A) whole-sample, (B) females only, (C) males only.

Table 2 – Regional volumetric comparisons in separate sexes. Data are presented separately for males and females. For each ROI, the means and SDs of right and left hemisphere cortical volume (mm^3) measurements are listed.

ROI	Males			Females		
	Mean (SD)		Sig.	Mean (SD)		Sig.
	Left (mm^3)	Right (mm^3)		Left (mm^3)	Right (mm^3)	
Anterior occipital sulcus	1092 (272.3)	950.6 (257.8)	n.s.	1103.1 (283.9)	838.1 (332.8)	<.05[a]
Calcarine sulcus	3462.6 (698)	4012.5 (736.4)	<.05[a]	3296.8 (600.3)	3789.1 (680.1)	<.05[a]
Central insular sulcus	309.8 (73.4)	274.7 (58.5)	n.s.	267.4 (84.8)	241.4 (83.8)	n.s.
Central sulcus	3675.9 (596.9)	3670.5 (712.4)	n.s.	3539.9 (353.4)	3297.5 (484.6)	n.s.
Cingulate and intracingulate sulci	7042.7 (1030.4)	10100.4 (1375.1)	<.05[a]	6540.2 (820)	8919.5 (1106.8)	<.05[a]
Cingulate gyrus	5140.9 (836.4)	4133.2 (729.2)	<.05[a]	4319.6 (936.3)	3817.1 (670.3)	n.s.
Cingulate sulcus (marginalis part)	1390.7 (209.8)	1393.1 (331.4)	n.s.	1270.4 (297.3)	1227.7 (266.7)	n.s.
Circular sulcus of insula (anterior)	1009.2 (134.8)	1153.6 (313.7)	n.s.	857.9 (134.3)	941.7 (147.1)	n.s.
Circular sulcus of insula (inferior)	2417.7 (315.2)	2020.5 (271.6)	<.05[a]	2174.4 (310.2)	1790.5 (220)	<.05[a]
Circular sulcus of insula (superior)	2928.6 (366.8)	2259.9 (348.5)	<.05[a]	2619.6 (303.2)	2135.5 (293)	<.05[a]
Collateral transverse sulcus (anterior)	1548.2 (334.1)	1657.7 (557.5)	n.s.	1497 (447)	1689.5 (381.1)	n.s.
Collateral transverse sulcus (posterior)	522.5 (184.5)	828.4 (218.7)	<.05[a]	461.6 (113.8)	693.4 (188)	<.05[a]
Cuneus	3631.2 (480)	3575.4 (783.5)	n.s.	3171.5 (524.8)	3214.3 (430.9)	n.s.
Frontomarginal gyrus	1154.7 (279.1)	1331.5 (343.5)	n.s.	903.3 (249.5)	1054.9 (208.4)	n.s.
Frontomarginal sulcus	1077.7 (252.4)	805.2 (211.3)	n.s.	931.4 (236.5)	721.6 (159.6)	n.s.
Gyrus rectus	2318.7 (328.2)	1800 (310.4)	<.05[a]	1981.5 (317.3)	1531.3 (227.7)	<.05[a]
H-shaped orbital sulcus	2573.1 (435.9)	2538.3 (433.2)	n.s.	2427.3 (342.8)	2312.3 (337.3)	n.s.
Inferior frontal gyrus (opercular part)	3608.3 (766.2)	3252.9 (523.2)	n.s.	3181.1 (426.6)	3043.2 (470.6)	n.s.
Inferior frontal gyrus (orbital part)	907.8 (262.4)	989.3 (271.4)	n.s.	832.3 (218.2)	878.3 (175.5)	n.s.
Inferior frontal gyrus (triangular part)	2809.5 (520)	2880.6 (537.6)	n.s.	2581.6 (345.9)	2519.7 (504.9)	n.s.
Inferior frontal sulcus	3274 (960.3)	3085 (582.1)	n.s.	2920 (376.7)	2845.6 (312.2)	n.s.
Inferior occipital gyrus and sulcus	2997.7 (744.8)	2953 (578.9)	n.s.	2585.8 (640)	2706.5 (669.2)	n.s.
Inferior parietal gyrus (angular part)	5673.6 (872.9)	7436.8 (1005.8)	<.05[a]	5390.3 (862.3)	6431.2 (1044.2)	<.05[a]
Inferior parietal gyrus (supramarginal part)	7077.1 (1204)	6718 (1118)	n.s.	6244.3 (1001.9)	6200 (834.2)	n.s.
Inferior temporal gyrus	6877.1 (1152.9)	6610.4 (1209.7)	n.s.	5821.7 (1558)	5823.5 (1330.7)	n.s.
Inferior temporal sulcus	2104.4 (452.3)	1949.2 (436.8)	n.s.	1832.8 (495.2)	1629.3 (399.5)	n.s.
Insular gyrus (long)	880.1 (160.8)	925.2 (182.7)	n.s.	860.2 (321)	821.1 (148)	n.s.
Insular gyrus (short)	1966.4 (312.4)	1931 (315)	n.s.	1733.1 (304.5)	1613 (327.4)	n.s.
Intraparietal and transverse parietal sulci	3972.5 (538.7)	4225.4 (652.1)	n.s.	3651 (461.9)	3807.9 (406.5)	n.s.
Isthmus	373.6 (117.6)	412.4 (118.6)	n.s.	328 (78.3)	336.2 (57.4)	n.s.
Lateral fissure (horizontal ramus)	528.7 (160)	607 (147.7)	n.s.	467.7 (115.3)	548.6 (87.4)	n.s.
Lateral fissure (posterior)	1683.7 (313.7)	2071.6 (277.5)	<.05[a]	1590 (216.9)	1859.1 (163.8)	<.05[a]
Lateral fissure (vertical ramus)	602.7 (159.3)	413.6 (139.2)	n.s.	593.9 (178.5)	457.8 (139.9)	n.s.
Lateral occipito-temporal gyrus (fusiform)	4629.9 (691)	4588.8 (773.3)	n.s.	4409.4 (812.7)	3775.3 (614.3)	n.s.
Lateral orbital gyrus	6686 (964.1)	7314.6 (1339.5)	n.s.	5812.7 (842.4)	6262.6 (729.5)	n.s.
Lateral orbital sulcus	691.4 (218)	790.7 (364.4)	n.s.	562.9 (160.2)	660.7 (199.8)	n.s.
Lingual gyrus	5917.4 (979.4)	6750.1 (984.9)	n.s.	5286.3 (773.6)	6331.9 (911.2)	<.05[a]
Medial occipito-temporal and lingual sulci	3334.1 (492.3)	3461.4 (758.6)	n.s.	3032.6 (625.8)	2898.8 (352.8)	n.s.
Medial occipito-temporal gyrus (parahippocampal part)	4443.2 (547.1)	4657.3 (514.7)	n.s.	4031.9 (517.8)	4323.1 (555.2)	n.s.
Medial orbital sulcus	960.8 (152.5)	914 (203.5)	n.s.	862.8 (132.8)	799.6 (112.5)	n.s.
Medial wall	5954.4 (900.2)	5731.4 (551.7)	n.s.	5110.9 (1105.3)	5283.2 (839.5)	n.s.
Middle frontal gyrus	10194.3 (2124.6)	10775.8 (2222.3)	n.s.	9041.1 (1580.6)	9618 (1087.8)	n.s.
Middle occipital gyrus	4560.4 (585.1)	4793.6 (816.1)	n.s.	4254.2 (545.2)	4320.2 (575.4)	n.s.
Middle occipital sulcus and sulcus lunatus	1576.1 (381.3)	1696.4 (491.6)	n.s.	1522.6 (467.6)	1476.7 (568.3)	n.s.
Middle temporal gyrus	8750.1 (1118.5)	9180 (1223.2)	n.s.	7474.8 (1324.1)	7778.9 (1123)	n.s.
Occipito-temporal sulcus (lateral)	1410.3 (311.2)	1482.6 (373.5)	n.s.	1242.7 (338.5)	1341 (289)	n.s.
Paracentral gyrus	2692.2 (368.1)	2187.8 (302.7)	<.05[a]	2410.2 (420.3)	2011.7 (432.7)	<.05[a]
Paracentral sulcus	329 (103.9)	300.2 (73.2)	n.s.	307.5 (84.3)	248.8 (89.9)	n.s.
Parieto-occipital sulcus	2836 (541.8)	2962.5 (433.4)	n.s.	2440.7 (472.7)	2686.6 (530.6)	n.s.
Pericallosal sulcus	1367.4 (185.9)	1637.4 (259.8)	<.05[a]	1236 (220.1)	1544.4 (290.3)	<.05[a]
Planum polare	1930.8 (425.7)	2051.8 (440.6)	n.s.	1812.9 (344.2)	1843.2 (332)	n.s.
Planum temporale	2407.9 (581.6)	1889.6 (379.4)	<.05[a]	2172.7 (356.4)	1885.5 (352.5)	n.s.
Postcentral gyrus	4212.6 (775.2)	3691.4 (715.1)	<.05[a]	4189.2 (577.2)	3413.8 (695.2)	<.05[a]
Postcentral sulcus	4077.7 (652.3)	3292.3 (858)	<.05[a]	3497.1 (506.3)	2706.4 (503.7)	<.05[a]
Precentral gyrus	6533.2 (884.7)	6609.1 (1009.6)	n.s.	5945.6 (653.4)	5792.9 (711.6)	n.s.
Precentral sulcus (inferior part)	2544.3 (636)	2665 (370.5)	n.s.	2403.7 (502)	2564.9 (248.8)	n.s.
Precentral sulcus (superior part)	2083.9 (552)	2239.4 (356.1)	n.s.	1775.2 (296.2)	1876.1 (359.8)	n.s.
Precuneus gyrus	5590.3 (929.6)	5663.8 (986.3)	n.s.	4942.4 (461.5)	4887.9 (446.9)	n.s.
Subcallosal gyrus	318.8 (155.1)	244.3 (85.5)	n.s.	312.3 (136.3)	269.6 (77.8)	n.s.

Table 2 – (*continued*)

ROI	Males			Females		
	Mean (SD)		Sig.	Mean (SD)		Sig.
	Left (mm^3)	Right (mm^3)		Left (mm^3)	Right (mm^3)	
Subcentral gyrus	2625.2 (482.1)	2011.2 (400.1)	<.05[a]	2519.8 (279.2)	1960.3 (380.6)	<.05[a]
Subcentral sulcus (anterior)	168.8 (95)	301.6 (107.5)	n.s.	157.4 (72.2)	273.5 (112.6)	n.s.
Subcentral sulcus (posterior)	534.4 (146.5)	454.4 (107)	n.s.	462.9 (144.9)	424.7 (139.7)	n.s.
Suborbital sulcus	1096 (262.8)	704.2 (184.8)	<.05[a]	914.8 (201.9)	525.5 (139.9)	<.05[a]
Subparietal sulcus	1765.3 (416.6)	2190.8 (539)	<.05[a]	1619.1 (228.8)	1967.2 (403.3)	n.s.
Sulcus intermedius primus (Jensen)	606.2 (265.4)	811.3 (326.8)	n.s.	483.1 (231.7)	591.7 (146.5)	n.s.
Superior frontal gyrus	21154.3 (3018.9)	19435.4 (2431.2)	<.05[a]	19094.9 (2106.8)	17487.1 (1978.6)	<.05[a]
Superior frontal sulcus	5054.1 (971.2)	4238.2 (987.4)	<.05[a]	4521.4 (921.4)	3924.1 (815.7)	n.s.
Superior occipital gyrus	2620.8 (489.4)	3457.7 (536.6)	<.05[a]	2281.2 (340.7)	2720.2 (439.6)	<.05[a]
Superior occipital sulcus and sulcus transversalis	1712 (354.6)	1807.6 (397.4)	n.s.	1584.1 (291.3)	1822.9 (245.1)	n.s.
Superior parietal gyrus	6141 (944.5)	5011 (745.6)	<.05[a]	5307.7 (837.6)	4467.3 (586.5)	<.05[a]
Superior temporal gyrus (lateral aspect)	6205.8 (902.2)	5509 (727.7)	n.s.	5593.4 (659.6)	4747.8 (664.2)	<.05[a]
Superior temporal sulcus	9046.6 (1251.5)	10057.2 (1069)	n.s.	8520.5 (1278.1)	9255.6 (1116.8)	n.s.
Temporal pole	5982.5 (642.5)	5987.8 (612.6)	n.s.	5211.9 (847.7)	5393.4 (619.1)	n.s.
Transverse temporal gyrus and intermediate sulcus	1124.6 (238.6)	872.7 (213.9)	<.05[a]	1048.6 (162.8)	807.5 (147)	<.05[a]
Transverse temporal sulcus	563.2 (155.1)	457.5 (111.3)	n.s.	497.7 (109.8)	455.9 (91.5)	n.s.

a After Bonferroni correction for multiple comparisons.

may be important for refining our understanding of hemispheric specialization. Inferoparietal association cortex, near the boundary of temporal and parietal lobes, helps maintain attention to the outside world (Corbetta and Shulman, 2002), and its damage, particularly on the right side, results in attentional impairment (Heilman et al., 2003). Prefrontal cortex found on the lateral aspect of the hemisphere (dorsolateral and ventrolateral) is critical for accessing and activating task-relevant representations found in the posterior association cortices (O'Reilly and Munakata, 2000; Jonides et al., 2008; Van Snellenberg and Wager, 2009). Close neuroanatomical connectivity and functional relationship exists between the posterior heteromodal association cortices and lateral prefrontal heteromodal association cortices (Goldman-Rakic, 1988; Fuster, 2008). By contrast, mesial/orbitomesial prefrontal and anterior cingulate cortices (ACCs) are critical for salience-driven decision making guided to a large extent by the organisms's internal states, motivations and needs (Bechara et al., 1998; Koenigs et al., 2007; Botvinick et al., 1999; Carter et al., 1999). The functional implications of the dual lateral versus mesial heteromodal association cortical asymmetry with opposite and complementary cortical space allocation are intriguing and they await further clarification. A possible relationship between hemispheric differences in heteromodal versus modality-specific cortical space allocation and the differential roles of the two hemispheres in learning was ascertained in the old literature (Goldberg and Costa, 1981), but it clearly requires a re-examination with modern methodology.

4.2. *Modality-specific cortical asymmetries*

We also found hemispheric differences in the modality-specific cortical regional volumes. Areas implicated in visual processing are more extensive in the right than left hemisphere. By contrast, somatosensory cortex, auditory cortex, portions of premotor cortex, and motor cortices controlling oropharyngeal structures are more extensive in the left than right hemisphere. Our findings that the superior temporal gyrus, *planum temporale*, and inferior portion of the motor areas are volumetrically larger in the left than right hemisphere parallel previously reported asymmetries in the *planum temporale* and frontal operculum (Geschwind and Levitsky, 1968; Galaburda et al., 1978). Luders et al. (2006) reported a similar pro-left hemispheric asymmetry in the cortical thickness of anterior temporal-lobe structures. Our finding of pro-right hemispheric differences in the volume of cortex implicated in visual processing parallels the cortical surface differences reported by Lyttelton et al. (2009) and cortical thickness differences reported by Luders et al. (2006). These asymmetries are broadly consistent with the commonly described left hemispheric dominance for language and right hemispheric dominance for visuo-spatial processing in humans.

4.3. *Cortical space allocation on the lateral versus mesial aspects of the hemispheres*

Cortical space allocation on the lateral (convexital) aspect appears to follow a relatively clear pattern. Heteromodal association cortices are more extensively represented in the right than in the left hemisphere. We found this to be true both for the prefrontal and for the inferoparietal cortices. By contrast, modality-specific cortices are more extensively represented in the left than in the right hemisphere. Our data confirmed this for somatosensory cortex, auditory cortex, portions of premotor cortex, and motor cortices controlling oropharyngeal structures. This is consistent with the earlier predictions (Goldberg and Costa, 1981).

We found that cortical space allocation on the mesial aspect appears to be characterized by a more extensive representation of the orbital and mesial frontal and cingulate cortices in the left than right hemisphere.

4.4. *Sex-linked differences*

Functional lateralization of the brain is present both in females and in males and is controlled by multiple factors (Liu et al., 2009). Examination of sex-linked differences in cortical morphology was not the primary focus of this study and any such differences reported here should be viewed as preliminary and requiring confirmation with larger samples. Nonetheless, our findings suggest volumetric asymmetry in the cingulate cortex (left larger than right) in males but not in females. The functional implications of this asymmetry is unclear, but it does parallel the sex-linked differences in the effects of lateralized prefrontal lesions on response selection in an intentionally underconstrained, ambiguous perceptual preference tasks devoid of intrinsic "true-false" metric (Goldberg et al., 1994a, 1994b; Goldberg and Podell, 1999). In right-handed females, both left and right frontal lesions shift responses toward extreme dependence on the perceptual context, making them excessively changeable compared to healthy controls. In right-handed males right frontal lesions shift responses toward extreme context dependence, but left frontal lesions – toward extreme context independence characterized by excessively stable responses.

These sex-linked differences in the lateralized prefrontal lesion effects on response selection parallel our findings of sex-linked differences in the relative sizes of the left and right ACC: they are symmetric in females and asymmetric in males. ACC plays a role in resolving situations characterized by uncertainty and ambiguity (Krain et al., 2006; Pushkarskaya et al., 2010). Sex-linked differences in the degree of lateralization of the frontal-lobe control over response selection in ambiguous, underdetermined situations may be a consequence of sex-linked differences in the degree of structural ACC asymmetries. While ACC is not the only structure implicated in decision making under ambiguity – so are the orbitofrontal and mesial frontal areas – the fact that the sex-linked differences in decision making in ambiguous environments parallel the anatomical findings in ACC but not in the other regions may suggest a particularly central role of ACC in resolving ambiguity.

4.5. *Limitations and future directions*

Replication of our findings, particularly as they pertain to sex-linked differences, needs to be conducted with a larger sample. The generalizability of our findings across lifespan is unclear at this time, since changes in morphological hemispheric asymmetries with age have been reported (Raz et al., 2004; Shaw et al., 2009). Thus replications in different age groups are important.

Further elucidation of the relationship of hemispheric asymmetries described here and neurological/neuropsychiatric disorders is another promising direction. Several neurological and neuropsychiatric disorders are characterized by asymmetric regional structural or physiological abnormalities, notably schizophrenia (Chance et al., 2008; Schobel et al., 2009; Wolf et al., 2008) and fronto-temporal dementia (Boccardi et al., 2003; Jeong et al., 2005; Kanda et al., 2008; Whitwell et al., 2005). The findings presented in this paper may help shed further light on the nature and implications of such asymmetries in these disorders.

Several patterns of hemispheric asymmetries described in this paper are particularly intriguing. These include the dual asymmetry of lateral versus mesial heteromodal association cortices, and the asymmetry of cortical space allocation between heteromodal association and modality specific association cortices on the lateral (convexital) aspects of the two hemispheres. In this paper we presented morphometric findings without any correlated neuropsychological data. Future studies may attempt to correlate the degree of expression of the asymmetries described here in healthy individuals with cognitive variables.

Analytic or computational models may also be illuminating in understanding complex structure–function relations. The differences in cortical space allocation to heteromodal versus modality-specific cortices can be relatively readily represented in formal models. It may be possible to clarify the functional ramifications of the asymmetries in cortical space allocation described in this paper computationally, by modeling them in multilayered neural net architectures and examining the effects of parametric variations within the models on learning (for a more detailed outline of this approach see Goldberg, 2009).

In conclusion, despite the prodigious body of work on hemispheric specialization, the riddle is far from solved, and more interdisciplinary work is needed, combining neuropsychological, neuroimaging, computational, genetic, and clinical approaches into a coordinated research effort.

REFERENCES

Anderson B, Southern BD, and Powers RE. Anatomic asymmetries of the posterior superior temporal lobes: A postmortem study. *Neuropsychiatry, Neuropsychology, and Behavioral Neurology*, 12(4): 247–254, 1999.

Beaton AA. The relation of planum temporale asymmetry and morphology of the corpus callosum to handedness, gender, and dyslexia: A review of the evidence. *Brain and Language*, 60(2): 255–322, 1997.

Bechara A, Damasio H, Tranel D, and Anderson SW. Dissociation of working memory from decision making within the human prefrontal cortex. *Journal of Neuroscience*, 18(1): 428–437, 1998.

Blackmon T, Barr WB, Kuzniecky R, DuBois J, Carlson CE, Quinn BT, et al. Phonetically irregular word pronunciation and cortical thickness in the adult brain. *NeuroImage*, 51(4): 1453–1458, 2010.

Boccardi M, Laakso MP, Bresciani L, Galluzi S, Geroldi C, Beltramello A, et al. The MRI pattern of frontal and temporal brain atrophy in fronto-temporal dementia. *Neurobiology of Aging*, 24(1): 95–103, 2003.

Botvinick M, Nystrom LE, Fissel K, Carter CS, and Cohen JD. Conflict monitoring versus selection-for-action in anterior cingulate cortex. *Nature*, 402(6758): 179–181, 1999.

Carter CS, Botvinick M, and Cohen JD. The contribution of the anterior cingulate cortex to executive processes in cognition. *Reviews in Neuroscience*, 10(1): 49–57, 1999.

Chance SA, Casanova MF, Switala AE, and Crow TJ. Auditory cortex asymmetry, altered minicolumn spacing and absence of ageing effects in schizophrenia. *Brain*, 131(12): 3178–3192, 2008.

Corbetta M and Shulman GL. Control of goal-directed and stimulus-driven attention in the brain. *Nature Reviews Neuroscience*, 3(3): 201–215, 2002.

Crespo-Facorro B, Roiz-Santiáñez R, Pérez-Iglesias R, Mata I, Rodríguez-Sánchez JM, Tordesillas-Gutiérrez D, et al. Sex-specific variation of MRI-based cortical morphometry in adult healthy volunteers: The effect on cognitive functioning. *Progress in Neuro-Psychopharmacology & Biological Psychiatry*, 35(2): 616–623, 2001.

Dale AM, Fischl B, and Sereno MI. Cortical surface-based analysis. I. Segmentation and surface reconstruction. *NeuroImage*, 9(2): 179–194, 1999.

Destrieux C, Fischl B, Dale AM, and Halgren E. A sulcal depth-based anatomical parcellation of the cerebral cortex. *NeuroImage*, 47(S1): S151, 2009.

Destrieux C, Fischl B, Dale A, and Halgren E. Automatic parcellation of human cortical gyri and sulci using standard anatomical nomenclature. *NeuroImage*, 53(1): 1–15, 2010.

Draganski B, Gaser C, Busch V, Schuierer G, Bogdahn U, and May A. Neuroplasticity: Changes in grey matter induced by training. *Nature*, 427(6972): 311–312, 2004.

Fischl B and Dale AM. Measuring the thickness of the human cerebral cortex from magnetic resonance images. *Proceedings of the National Academy of Sciences of the United States of America*, 97(20): 11050–11055, 2000.

Fischl B, Sereno MI, Tootell RB, and Dale AM. High-resolution intersubject averaging and a coordinate system for the cortical surface. *Human Brain Mapping*, 8(4): 272–284, 1999.

Fischl B, Liu A, and Dale AM. Automated manifold surgery: Constructing geometrically accurate and topologically correct models of the human cerebral cortex. *IEEE Transactions on Medical Imaging*, 20(1): 70–80, 2001.

Fischl B, van der Kouwe A, Destrieux C, Halgren E, Ségonne F, Salat DH, et al. Automatically parcellating the human cerebral cortex. *Cerebral Cortex*, 14(1): 11–22, 2004.

Fleming SM, Weil RS, Nagy Z, Dolan RJ, and Rees G. Relating introspective accuracy to individual differences in brain structure. *Science*, 329(5998): 1514–1543, 2010.

Fornito A, Yucel M, Wood S, Stuart GW, Buchanan JA, Proffitt T, et al. Individual differences in anterior cingulate/paracingulate morphology are related to executive functions in healthy males. *Cerebral Cortex*, 14(4): 424–431, 2004.

Foundas AL, Leonard CM, Gilmore R, Fennel E, and Heilman KM. Planum temporal asymmetry and language dominance. *Neuropsychologia*, 32(10): 1225–1231, 1994.

Foundas AL, Leonard CM, and Heilman KM. Morphologic cerebral asymmetries and handedness: The pars triangularis and planum temporale. *Archives of Neurology*, 52(5): 501–508, 1995.

Fuster JM. *The Prefrontal Cortex*. 4th ed. NY: Academic Press, 2008.

Galaburda AM, LeMay M, Kemper TL, and Geschwind N. Right-left asymmetries in the brain. *Science*, 199(4331): 852–856, 1978.

Geschwind N and Levitsky W. Human brain: Left-right asymmetries in temporal speech region. *Science*, 161(837): 186–187, 1968.

Gold JM, Berman KF, Randolph C, Goldberg TE, and Weinberger DR. PET validation of a novel prefrontal task: Delayed response alteration. *Neuropsychology*, 10(1): 3–10, 1996.

Goldberg E. *The New Executive Brain: Frontal Lobes in a Complex World*. NY: Oxford University Press, 2009.

Goldberg E and Costa LD. Hemisphere differences in the acquisition and use of descriptive systems. *Brain and Language*, 14(1): 144–173, 1981.

Goldberg E and Podell K. Adaptive versus veridical decision making and the frontal lobes. *Consciousness and Cognition*, 8(3): 364–377, 1999.

Goldberg E, Harner R, Lovell M, Podell K, and Riggio S. Cognitive bias, functional cortical geometry, and the frontal lobes: Laterality, sex, and handedness. *Journal of Cognitive Neuroscience*, 6(3): 276–296, 1994a.

Goldberg E, Podell K, and Lovell M. Lateralization of frontal lobe functions and cognitive novelty. *Journal of Neuropsychiatry and Clinical Neurosciences*, 6(4): 371–378, 1994b.

Goldman-Rakic PS. Topography of cognition: Parallel distributed networks in primate association cortex. *Annual Review of Neuroscience*, 11: 137–156, 1988.

Good CD, Johnsrude I, Ashburner J, Henson RNA, Friston KJ, and Frackowiak RSJ. Cerebral asymmetry and the effects of sex and handedness on brain structure: A voxel-based morphometric analysis of 465 normal adult human brains. *NeuroImage*, 14(3): 685–700, 2001.

Habib M, Gayraud D, Oliva A, Regis J, Salamon G, and Khalil R. Effects of handedness and sex on the morphology of the corpus callosum: A study with brain magnetic resonance imaging. *Brain and Cognition*, 16(1): 41–61, 1991.

Heilman KH, Watson RT, and Valenstein E. Neglect and related disorders. In Heilman KH and Valenstein E (Eds), *Clinical Neuropsychology*. 4th ed. NY: Oxford University Press, 2003: 296–346.

Henson R, Shallice T, and Dolan R. Neuroimaging evidence for dissociable forms of repetition priming. *Science*, 287(5456): 1269–1272, 2000.

Huster RJ, Westerhausen R, Kreuder F, Schwieger E, and Wittling W. Morphologic asymmetry of the human anterior cingulate cortex. *NeuroImage*, 34(3): 888–895, 2007.

Jeong Y, Cho SS, Park JM, Kang SJ, Lee JS, Kang E, et al. 18F-FDG PET findings in frontotemporal dementia: An SPM analysis of 29 patients. *Journal of Nuclear Medicine*, 46(2): 233–239, 2005.

Jonides J, Lewis RL, Nee DE, Lustig CA, Berman MG, and Moore KS. The mind and brain of short-term memory. *Annual Review of Psychology*, 59: 193–224, 2008.

Kamiya Y, Aihara M, Osada M, Ono C, Hatakeyama K, Kanemura H, et al. Electrophysiological study of lateralization in the frontal lobes (in Japanese). *Japanese Journal of Cognitive Neuroscience*, 3(3): 188–191, 2002.

Kanda T, Ishii K, Uemura T, Miyamoto N, Yoshikawa T, Kono AK, et al. Comparison of grey matter and metabolic reductions in frontotemporal dementia using FDG-PET and voxel-based morphometric MR studies. *European Journal of Nuclear Medicine and Molecular Imaging*, 35(12): 2227–2234, 2008.

Koenigs M, Young L, Adolphs R, Tranel D, Cushman F, Hauser M, et al. Damage to the prefrontal cortex increases utilitarian moral judgments. *Nature*, 446(7138): 908–911, 2007.

Krain AL, Wilson AM, Arbuckle R, Castellanos FX, and Milham MP. Distinct neural mechanisms of risk and ambiguity: A meta-analysis of decision-making. *NeuroImage*, 32(1): 477–484, 2006.

LeMay M and Culebras A. Human brain - morphological differences in the hemispheres demonstrable by carotid arteriography. *New England Journal of Medicine*, 287(4): 168–170, 1972.

Liu H, Stufflebeam SM, Sepulcre J, Hedden T, and Buckner RL. Evidence from intrinsic activity that asymmetry of the human brain is controlled by multiple factors. *Proceedings of the National Academy of Sciences of the United States of America*, 106(48): 20499–20503, 2009.

Luders E, Narr KL, Thompson PM, Rex DE, Jäncke L, and Toga AW. Hemispheric asymmetries in cortical thickness. *Cerebral Cortex*, 16(8): 1232–1238, 2006.

Luders E, Gaser C, Narr KL, and Toga AW. Why sex matters: Brain size independent differences in gray matter distributions

between men and women. *Journal of Neuroscience*, 29(45): 14265–14270, 2009.
Lyttelton OC, Karama S, Ad-Dab'bagh Y, Zatorre RJ, Carbonell F, Worsley K, et al. Positional and surface area asymmetry of the human cerebral cortex. *NeuroImage*, 46(4): 895–903, 2009.
Maguire EA, Gadian DG, Johnstrude IS, Good CD, Ashburner J, Frakowiak RS, et al. Navigation-related structural change in the hippocampi of taxi drivers. *Proceedings of the National Academy of Sciences of the United States of America*, 97(8): 4398–4403, 2000.
Nagata SI, Uchimura K, Hirakawa W, and Kuratsu JI. Method for quantitatively evaluating the lateralization of linguistic function using functional MR imaging. *American Journal of Neuroradiology*, 22(5): 985–991, 2001.
Narr KL, Bilder RM, Luders E, Thompson PM, Woods RP, Robinson D, et al. Asymmetries of cortical shape: Effects of handedness, sex and schizophrenia. *NeuroImage*, 34(3): 939–948, 2007.
Oldfield RC. The assessment and analysis of handedness: The Edinburgh inventory. *Neuropsychologia*, 9(1): 97–113, 1971.
O'Reilly RC and Munakata Y. *Computational Explorations in Cognitive Neuroscience*. Cambridge, MA: MIT Press, 2000.
Penhune VB, Zatorre RJ, MacDonald JD, and Evans AC. Interhemispheric anatomical differences in human primary auditory cortex: Probabilistic mapping and volume measurement from magnetic resonance scans. *Cerebral Cortex*, 6(5): 661–672, 1996.
Pushkarskaya H, Liu X, Smithson M, and Joseph JE. Beyond risk and ambiguity: Deciding under ignorance. *Cognitive, Affective, & Behavioral Neuroscience*, 10(3): 382–391, 2010.
Raz N, Gunning-Dixon F, Head D, Rodrigue KM, Williamson A, and Acker JD. Aging, sexual dimorphism, and hemispheric asymmetry of the cerebral cortex: Replicability of regional differences in volume. *Neurobiology of Aging*, 25(3): 377–396, 2004.
Schneider P, Scherg M, Dosch HG, Specht HJ, Gutschalk A, and Rupp A. Morphology of Heschl's gyrus reflects enhanced activation in the auditory cortex of musicians. *Nature Neuroscience*, 5(7): 688–694, 2002.
Schobel SA, Kelly MA, Corcoran CM, Van Heertum K, Seckinger R, Goetz R, et al. Anterior hippocampal and orbitofrontal cortical structural brain abnormalities in association with cognitive deficits in schizophrenia. *Schizophrenia Research*, 114(1–3): 110–118, 2009.
Shadmehr R and Holcomb HH. Neural correlates of motor memory consolidation. *Science*, 277(5327): 821–825, 1997.
Shaw P, Lalonde F, Lepage C, Rabin C, Eckstrand K, Sharp W, et al. Development of cortical asymmetry in typically developing children and its disruption in attention-deficit/hyperactivity disorder. *Archives of General Psychiatry*, 66(8): 888–896, 2009.
Takao H, Abe O, Yamasue H, Aoki S, Sasaki H, Kasai K, et al. Gray and white matter asymmetries in healthy individuals aged 21–29 years: A voxel-based morphometry and diffusion tensor imaging study. *Human Brain Mapping*, 32(10): 1762–1773, 2011.
Vallortigara G. Comparative neuropsychology of the dual brain: A stroll through animals' left and right perceptual worlds. *Brain and Language*, 73(2): 189–219, 2000.
Vallortigara G and Rogers LJ. Survival with an asymmetrical brain: Advantages and disadvantages of cerebral lateralization. *Behavioral and Brain Sciences*, 28(4): 575–633, 2005.
Vallortigara G, Rogers LJ, and Bisazza A. Possible evolutionary origins of cognitive brain lateralization. *Brain Research Reviews*, 30(2): 164–175, 1999.
Van Snellenberg JX and Wager T. Cognitive and motivational functions of the human prefrontal cortex. In Christensen A-L, Goldberg E, and Bougakov D (Eds), *Luria's Legacy in the 21st Century*. NY: Oxford University Press, 2009: 30–61.
Watkins KE, Paus T, Lerch JP, Zijdenbos A, Collins DL, Neelin P, et al. Structural asymmetries in the human brain: A voxel-based statistical analysis of 142 MRI scans. *Cerebral Cortex*, 11(9): 868–877, 2001.
Whitwell JL, Sampson EL, Watt HC, Harvey RJ, Rossor MN, and Fox NC. A volumetric magnetic resonance imaging study of the amygdala in frontotemporal lobar degeneration and Alzheimer's disease. *Dementia and Geriatric Cognitive Disorders*, 20(4): 238–244, 2005.
Witelson SF. Hand and sex differences in the isthmus and genu of the human corpus callosum. *Brain*, 112(3): 799–835, 1989.
Wolf RC, Höse A, Frasch K, Walter H, and Vasic N. Volumetric abnormalities associated with cognitive deficits in patients with schizophrenia. *European Psychiatry*, 23(8): 541–548, 2008.
Yakovlev PI. A proposed definition of the limbic system. In Hockman CH (Ed), *Limbic System Mechanisms and Autonomic Function*. Springfield, IL: Charles C. Thomas, 1972: 241–283.
Yakovlev PI and Rakic P. Patterns of decussation of bulbar pyramids and distribution of pyramidal tracts on two sides of the spinal cord. *Transactions of the American Neurological Association*, 91: 366–367, 1966.